Quantum effects in atomic reflection

Sze Tan, Daniel Walls

J. Phys. II France **4** (1994) 1897–1912 NOVEMBER **1994**, PAGE 1897

Classification
Physics Abstracts
42.50 — 32.80P

Quantum effects in atomic reflection

Sze M. Tan and Daniel F. Walls

Physics Department, The University of Auckland, Private Bag 92019, Auckland, New Zealand

(Received 29 April 1994, received in final form 15 September 1994, accepted 23 September 1994)

Abstract. — In this paper we consider the effects of spontaneous emission on the problem of atomic reflection from an optical evanescent travelling wave. The atoms are assumed to be travelling so slowly that the external degrees of freedom of the atom need to be treated quantum mechanically. Spontaneous emission is modelled using a fully quantum mechanical model based on the quantum Monte Carlo technique which includes the effects of atomic recoil. The results of the simulation are compared with a semi-classical Monte Carlo simulation in which the atomic motion is treated classically and the internal state of the atom is assumed to follow the light-induced quasipotentials adiabatically between spontaneous emission events. The spontaneous emission leads to a broadening of the momentum distribution of the outgoing wave packet and mechanisms for this broadening are discussed.

1. Introduction.

With the recent interest in producing optical systems such as cavities for atomic de Broglie waves, the importance of having efficient optical elements such as atomic mirrors has become apparent. Atomic mirrors which are based on the repulsive potential created by an evanescent light field [1] have been experimentally realized by several groups [2-5]. To date, most analyses of such mirrors have been concerned with achieving high reflectivities and maintaining coherence throughout the interaction and have thus sought conditions for which spontaneous emission may be avoided [1, 6-8]. Consequently, large laser intensities and detunings are used. When spontaneous emission is important, it has been found experimentally by Seifert *et al.* [5] that the distribution of outgoing momenta can be substantially broader than one might estimate from a simple consideration of the atomic recoil during spontaneous emission. They present a semi-classical analysis for this broadening in which the internal atomic state is treated quantum mechanically but the external motion is treated classically. This gives good agreement with the experimental results for the parameters used. In this paper we use the method of Monte Carlo wave functions [9, 10] in order to investigate the effects of spontaneous emission on the distribution of outgoing momentum in the situation where both internal and external degrees of freedom of the atom are treated quantum mechanically. When the atomic beam

has a sufficiently well-defined momentum, it is no longer possible to treat each atom as being well-localized. Instead, a wavepacket must be used to represent the spatial atomic coherence. A Gaussian wavepacket is chosen as it has the minimum width in position space compatible with a specified momentum uncertainty. The analysis treats the time-dependent evolution of such atomic wavepackets as they interact with the field. The results of these simulations are compared with the semi-classical approach and we find that when the spatial extent of the atomic wave packet becomes comparable with the scale over which the light-induced potential varies, additional quantum mechanical effects become significant in determining the outgoing momentum distribution.

2. System dynamics without spontaneous emission.

Figure 1 is a schematic diagram of the configuration in which a beam of cold two-level atoms impinges at glancing incidence on the evanescent light field produced by the total internal reflection of an intense laser beam at the surface of a prism. We shall treat the light field classically, but use a quantum mechanical description for the internal and external degrees of freedom of the atom. When spontaneous emission is not present, the system Hamiltonian in the rotating wave and electric dipole approximations is

$$H = \frac{p^2}{2m} + \hbar\epsilon_1 |1\rangle\langle 1| + \hbar\epsilon_2 |2\rangle\langle 2| - \left[\int \mathbf{D}^{(-)}(\mathbf{r}) \cdot \mathbf{E}_{\mathrm{L}}^{(+)}(\mathbf{r}, t)\, \mathrm{d}^3\mathbf{r} + \mathrm{c.c.}\right] \tag{1}$$

where p is the centre of mass momentum of the two-level atoms with mass m, and $|1\rangle$ and $|2\rangle$ are the lower and upper atomic levels with energies $\hbar\epsilon_1$ and $\hbar\epsilon_2$ respectively. $\mathbf{D}^{(-)}(\mathbf{r})$ is the dipole moment operator of the atom which is given by

$$\mathbf{D}^{(-)}(\mathbf{r}) = \boldsymbol{\mu} |2\rangle\langle 1| \otimes |\mathbf{r}\rangle\langle \mathbf{r}|\, \delta(\mathbf{r} - \mathbf{r}_{\mathrm{a}}) \tag{2}$$

where $\boldsymbol{\mu}$ is the dipole moment vector and $\mathbf{r}_{\mathrm{a}}$ is the position of the atom. The electric field of the light is $\mathbf{E}_{\mathrm{L}}^{(+)}(\mathbf{r}, t)$ where

$$\mathbf{E}_{\mathrm{L}}^{(+)}(\mathbf{r}, t) = \mathbf{E}_0 F(y) \exp[i(k_{\mathrm{L}} z - \omega_{\mathrm{L}} t)] \tag{3}$$

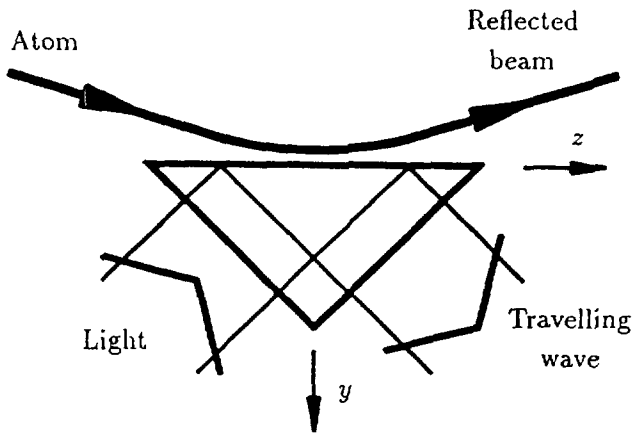

Fig. 1. — Atomic reflection from a travelling evanescent light field.

$F(y)$ specifies the transverse field profile, ω_L is the angular frequency and k_L is the wavenumber of the light.

Working in an interaction picture with free Hamiltonian $\hbar(\epsilon_1 + \omega_L)\,|2\rangle\langle 2| + \hbar\epsilon_1\,|1\rangle\langle 1|$ and defining the wave functions ϕ_1 and ϕ_2 *via*

$$|\psi\rangle = \int \mathrm{d}^3\mathbf{r}\,[\phi_1(\mathbf{r},t)\,|\mathbf{r}\rangle \otimes |1\rangle + \phi_2(\mathbf{r},t)\,|\mathbf{r}\rangle \otimes |2\rangle] \tag{4}$$

we obtain the Schrödinger equations

$$i\hbar\frac{\partial\boldsymbol{\phi}}{\partial t} = -\frac{\hbar^2}{2m}\left[\frac{\partial^2\boldsymbol{\phi}}{\partial y^2} + \frac{\partial^2\boldsymbol{\phi}}{\partial z^2}\right] + \begin{bmatrix} 0 & -\hbar\Omega F(y)\mathrm{e}^{-\imath k_L z}/2 \\ -\hbar\Omega F(y)\mathrm{e}^{\imath k_L z}/2 & -\hbar\Delta \end{bmatrix}\boldsymbol{\phi} \tag{5}$$

where $\Omega = 2\boldsymbol{\mu}\cdot\mathbf{E}_0/\hbar$ may be assumed to be real, $\Delta = \omega_L - (\epsilon_2 - \epsilon_1)$ is the detuning and $\boldsymbol{\phi}$ is a vector whose components are ϕ_1 and ϕ_2.

We now write $\boldsymbol{\phi}$ as a superposition of plane waves in the z direction so that

$$\boldsymbol{\phi}(\mathbf{r},t) = \frac{1}{2\pi\hbar}\int_{-\infty}^{\infty}\mathrm{d}k_z\,\boldsymbol{\varphi}(y,k_z,t)\mathrm{e}^{\imath k_z z} \tag{6}$$

Substituting this into the Schrödinger equation, we find that the ground state amplitude $\varphi_1(y,k_z,t)$ couples only to the excited state amplitude $\varphi_2(y,k_z+k_L,t)$ and *vice versa*. Thus, for each value of k_z we have the coupled equations

$$i\hbar\frac{\partial}{\partial t}\varphi_1(y,k_z,t) = -\frac{\hbar^2}{2m}\left[\frac{\partial^2}{\partial y^2} - k_z^2\right]\varphi_1(y,k_z,t) - \frac{1}{2}\hbar\Omega F(y)\varphi_2(y,k_z+k_L,t) \tag{7}$$

$$i\hbar\frac{\partial}{\partial t}\varphi_2(y,k_z+k_L,t) = \left\{-\frac{\hbar^2}{2m}\left[\frac{\partial^2}{\partial y^2} - (k_z+k_L)^2\right] - \hbar\Delta\right\}\varphi_2(y,k_z+k_L,t) - \frac{1}{2}\hbar\Omega F(y)\varphi_1(y,k_z,t) \tag{8}$$

If we consider atoms incident in the ground state with well-defined $k_z = k_I$, it is only necessary to deal with the vector $\boldsymbol{\varphi}(y,t)$ whose components are $\varphi_1(y,k_I,t)$ and $\varphi_2(y,k_I+k_L,t)$. We may remove a common phase factor $\exp[-i\hbar k_I^2 t/(2m)]$ from each component to obtain

$$i\hbar\frac{\partial}{\partial t}\boldsymbol{\varphi}(y,t) = -\frac{\hbar^2}{2m}\frac{\partial^2}{\partial y^2}\boldsymbol{\varphi}(y,t) + \begin{bmatrix} 0 & -\hbar\Omega F(y)/2 \\ -\hbar\Omega F(y)/2 & -\hbar(\Delta-\Delta_D) + E_R \end{bmatrix}\boldsymbol{\varphi}(y,t) \tag{9}$$

where $\Delta_D = \hbar k_I k_L/m$ is the Doppler shift seen by the atom due to its motion in the light and $E_R = \hbar^2 k_L^2/(2m)$ is the recoil energy which is usually very small.

3. Quantum Monte Carlo approach to spontaneous emission.

The quantum Monte Carlo wave function approach to treating spontaneous emission is described in detail by Dum, Zoller and Ritsch [9] and by Molmer, Castin and Dalibard [10]. Instead of using a density matrix to represent the mixed state of the system, a conditional wave function is introduced which describes the state of the system conditioned on a particular history of photodetections. An ensemble of photodetection histories is generated using random numbers and the time-evolution of a particular conditional wave function is referred to as a quantum trajectory. By calculating ensemble averages over these quantum trajectories, the

expectation values of all quantities tend to those found calculated using density matrices and the master equation.

As discussed by Molmer *et al.* [10], the quantum Monte Carlo technique allows us to include Liouvillians of the form

$$\mathcal{L}\rho = \sum_m C_m \rho C_m^\dagger - \frac{1}{2} C_m^\dagger C_m \rho - \frac{1}{2} \rho C_m^\dagger C_m \tag{10}$$

This equation typically arises from linear couplings between system operators C_m and their respective baths. In the case of spontaneous emission, the various possible values of m represent the possible directions of propagation $\mathbf{k}$ and polarization $\mathbf{e}$ of the outgoing spontaneously emitted photon. We find that

$$C_{(\mathbf{k},\mathbf{e})} = \sqrt{\frac{3\Gamma}{8\pi}} (\mathbf{e}^* \quad \boldsymbol{\mu}) \exp(-i\mathbf{k}\cdot\mathbf{r}) |1\rangle \langle 2| \tag{11}$$

On the right-hand side, the first two factors represent how efficiently an atom with dipole moment $\boldsymbol{\mu}$ radiates spontaneously with polarization $\mathbf{e}$, the exponential represents the the momentum kick of $-\mathbf{k}$ imparted to the atom due to recoil and $|1\rangle \langle 2|$ is the operator which lowers the atom into the ground state.

In the quantum Monte Carlo algorithm, a quantum jump results in one of the "collapse operators" C_m being applied to the system wave function $|\psi(t)\rangle$. Between one quantum jump and the next, we adopt the following procedure [11]:

i) a random number r uniformly distributed in the interval $(0, 1)$ is generated;

ii) the wave function $|\psi(t)\rangle$ is evolved using a Schrödinger equation with the non-Hermitian Hamiltonian

$$H' = H - \frac{i\hbar}{2} \sum_m C_m^\dagger C_m \tag{12}$$

where H is the system Hamiltonian in the absence of the loss process. For the case of spontaneous emission, the sum becomes an integral over permitted directions and polarizations of the outgoing photon and this reduces to

$$H' = H - \frac{i\hbar\Gamma}{2} |2\rangle \langle 2| ; \tag{13}$$

iii) as this evolution proceeds, the norm of ψ decreases. When $\langle\psi|\psi\rangle = r$, a quantum jump is carried out. One of the collapse operators C_m is chosen according to probabilities proportional to $\langle\psi| C_m^\dagger C_m |\psi\rangle$. This collapse operator is applied to $|\psi\rangle$ and the result is renormalized. i.e., we set

$$|\psi\rangle \to \frac{C_m |\psi\rangle}{\sqrt{\langle\psi| C_m^\dagger C_m |\psi\rangle}} \tag{14}$$

At this stage a new random number is generated to find the time of the next quantum jump.

It is straightforward to calculate the relative probabilities $\langle\psi| C_m^\dagger C_m |\psi\rangle$ with which spontaneous emission occurs in different directions if we know how the atomic dipole moment $\boldsymbol{\mu}$ is aligned. If $\boldsymbol{\mu}$ is aligned with the driving light field, the probability of emission per unit solid angle $\mathrm{d}\Omega$ in direction $\mathbf{k}$ is proportional to

$$P(\Omega) \propto |\boldsymbol{\mu}\cdot\mathbf{e}_1|^2 + |\boldsymbol{\mu}\cdot\mathbf{e}_2|^2 \tag{15}$$

where $\mathbf{e}_1$ and $\mathbf{e}_2$ are two polarization vectors orthogonal to $\mathbf{k}$. The probability density is normalized to give an integral of unity when taken over all possible outgoing directions.

For a circularly polarized classical light field travelling along the z axis, we may suppose μ to be given by $|\mu|(\hat{\mathbf{x}} + i\hat{\mathbf{y}})/\sqrt{2}$. In order to find the probability of spontaneous emission per unit solid angle along the direction (θ, ϕ) in spherical polar coordinates, we consider $\mathbf{k} = |\mathbf{k}|[\sin\theta(\hat{\mathbf{x}}\cos\phi + \hat{\mathbf{y}}\sin\phi) + \hat{\mathbf{z}}\cos\theta]$. We may choose $\mathbf{e}_{1,2}$ to be any two unit vectors perpendicular to $\mathbf{k}$. A convenient choice is $(\hat{\boldsymbol{\theta}} \pm i\hat{\boldsymbol{\phi}})/\sqrt{2}$ where $\hat{\boldsymbol{\theta}} = \cos\theta(\hat{\mathbf{x}}\cos\phi + \hat{\mathbf{y}}\sin\phi) - \hat{\mathbf{z}}\sin\theta$ and $\hat{\boldsymbol{\phi}} = -\hat{\mathbf{x}}\sin\phi + \hat{\mathbf{y}}\cos\phi$. Evaluating the inner products in (15), we find

$$P(\Omega) \propto \frac{1}{4}[(\cos\theta + 1)^2 + (\cos\theta - 1)^2] \tag{16}$$

Normalizing this according to

$$\int_0^{2\pi} \int_0^{\pi} P(\theta, \phi) \sin\theta \, \mathrm{d}\theta \, \mathrm{d}\phi = 1 \tag{17}$$

yields

$$\Pr[\text{spontaneous emission into } \mathrm{d}\Omega] = \frac{3}{16\pi}(1 + \cos^2\theta)\, \mathrm{d}\Omega \tag{18}$$

It is now possible to use a random number generator to produce a direction (θ, ϕ) according to this distribution. The probability is independent of ϕ which is thus distributed uniformly in the range 0 to 2π. The cumulative distribution function for θ is given by

$$2\pi \int_0^{\theta} P(\theta', \phi) \sin\theta' \, \mathrm{d}\theta' = \frac{1}{2} - \frac{3}{8}\cos\theta - \frac{1}{8}\cos^3\theta \tag{19}$$

Given a random number distributed uniformly in the range 0 to 1, the above relationship is inverted to find a corresponding value of θ.

In a similar way, it is possible to show that for a linearly polarized classical light field, the probability of spontaneous emission depends on the angle ψ between the polarization direction of the incident field and the wave vector $\mathbf{k}$ of the emitted light. We find that

$$\Pr[\text{spontaneous emission into } \mathrm{d}\Omega] = \frac{3}{8\pi}\sin^2\psi \, \mathrm{d}\Omega \tag{20}$$

A random number generator can similarly be used to choose the direction of spontaneous emission in this case.

4. The semi-classical Monte Carlo algorithm.

A semi-classical algorithm was developed by Seifert *et al.* [5] in order to explain experimental results for atomic reflection off an evanescent wave mirror. In this model, the external motion of the particle is treated classically. The matrix in the Schrödinger equations of motion equation (9) may be regarded as defining a potential within which the atom is moving. The eigenvalues of the matrix are hence known as *quasipotentials* and the eigenvectors define the particular combinations (called the *dressed states*) of the internal atomic states which experience these potentials. The dressed states and quasipotentials depend on the intensity of the light field "seen" by the atom and if the rate of change of this intensity is sufficiently slow, an adiabatic following approximation [12] may be employed which states that the atom will "follow" a dressed state as the intensity changes slowly.

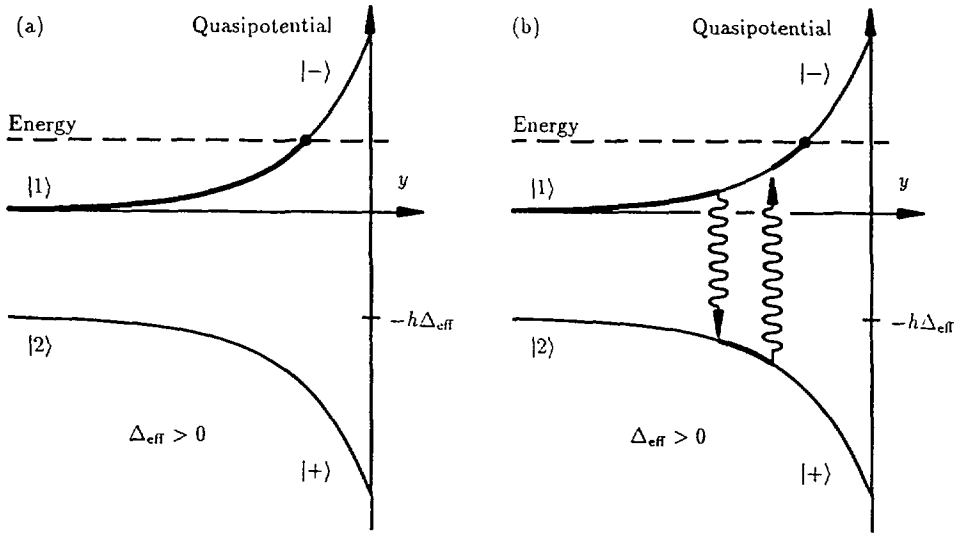

Fig. 2. — (a) Quasipotential curves and "path" of atom incident on mirror in the ground state, (b) transitions between dressed states caused by spontaneous emissions

The quasipotentials experienced by the atom are

$$U_{\pm}(y) = \frac{a \pm \sqrt{a^2 + 4b^2}}{2} \tag{21}$$

where $a = -\hbar(\Delta - \Delta_{\rm D}) + E_{\rm R}$ and $b = -\hbar\Omega F(y)/2$. The associated dressed states are

$$|-\rangle = \mathcal{N}_{-}\left[\frac{-a - \sqrt{a^2 + 4b^2}}{2b}|1\rangle + |2\rangle\right] \tag{22}$$

$$|+\rangle = \mathcal{N}_{+}\left[\frac{-a + \sqrt{a^2 + 4b^2}}{2b}|1\rangle + |2\rangle\right] \tag{23}$$

where $\mathcal{N}_{\pm}$ are normalization constants.

In the absence of the light ($F = 0$), the quasipotentials are $U_{-} = 0$ and $U_{+} = a$. The dressed state $|-\rangle$ corresponds to the ground state $|1\rangle$ and $|+\rangle$ to the excited state $|2\rangle$. The light-induced level shifts for low intensities $b \ll a/2$ is $\pm b^2/a$ which corresponds to the predictions of perturbation theory. For positive effective detuning ($\Delta_{\rm eff} = \Delta - \Delta_{\rm D} > 0$), we find that $a < 0$ and so the light raises the U_{-} quasipotential and lowers the U_{+} quasipotential. Atoms in the $|-\rangle$ dressed state are repelled and those in the $|+\rangle$ dressed state are attracted by regions of high intensity. The gradient force experienced by the atom is $-\partial U_{\pm}/\partial y$.

If an atom is initially in the ground state when it is far from the atomic mirror, it follows the dressed state $|-\rangle$ and experiences the gradient force $-\partial U_{-}/\partial y$. It is straightforward to integrate the classical equations of motion for this force law. Figure 2a shows the quasipotentials $U_{\pm}(y)$ for an evanescent wave. As the atom approaches the mirror, the $|-\rangle$ state contains a greater portion of the excited state $|2\rangle$, and the probability of being in the excited state is given by $P_{\rm e} = |\langle 2|-\rangle|^2 = \mathcal{N}_{-}^2$. The probability of a spontaneous emission in interval $\mathrm{d}t$ at time t is $\gamma P_{\rm e}(t)\mathrm{d}t$ where γ is the linewidth. The probability that no spontaneous emission occurs within

the interval 0 to T is thus given by

$$\Pr[\text{No spontaneous emission in } 0 < t < T] = \exp\left(-\int_0^T \gamma P_e(\tau)\,d\tau\right) \tag{24}$$

In order to find the time for a spontaneous emission, a random number r is generated which is uniformly distributed in $(0,1)$. An additional variable λ is integrated along with the position and velocity in accordance with the differential equation

$$\frac{d\lambda}{dt} = -\gamma P_e(t)\lambda \tag{25}$$

This is initialized to $\lambda(0) = 1$ and a spontaneous emission is deemed to occur once λ falls to the value of r. After each spontaneous emission, λ is reinitialized to one and a new random value of r is generated to determine the time of the next spontaneous emission.

The spontaneous emission results in two physical effects, the recoil imparted to the atom and the projection of the internal atomic state to the ground state. The direction of the emitted photon is chosen from the appropriate angular distribution and a momentum kick of $-\hbar\mathbf{k}_L$ is given to the atom. This changes the momentum but not the position of the atom. In the dressed state picture, the ground state is a linear superposition of the $|+\rangle$ and $|-\rangle$ states. In keeping with the semi-classical approach however, only one of these dressed states is selected with probabilities dependent on their overlap with the ground state. The atom is assumed to follow adiabatically the new dressed state and to be subject to the force $-\partial U_-/\partial y$ or $-\partial U_+/\partial y$ until the time of the next spontaneous emission.

As discussed by Seifert *et al.* [5], if the atom makes a transition to the $|+\rangle$ state, it experiences an attractive gradient force, which strongly deflects it towards the mirror. Unless a further spontaneous emission occurs, such an atom will be lost to the mirror surface. Figure 2b shows a possible semi-classical "path" for the atomic state, where the vertical transitions indicate spontaneous emissions. Atoms which are reflected can be deflected through large angles due to such large fluctuations in the force [13].

5. Solution of the quantum mechanical equations.

In order to include spontaneous emission, the evolution between quantum jumps is given by modifying the Hamiltonian according to equation (13) in the Schrödinger equation (9). The resulting equations are solved by a split-operator method [14] by separating the Hamiltonian into a part which is diagonal in momentum space and another which is diagonal in position space. The former is given by

$$H_A = -\frac{\hbar^2}{2m}\frac{\partial^2}{\partial y^2} + \begin{bmatrix} 0 & 0 \\ 0 & -\hbar\Delta_{\text{eff}} + E_R - i\hbar\gamma/2 \end{bmatrix} \tag{26}$$

$$= \begin{bmatrix} p_y^2/(2m) & 0 \\ 0 & p_y^2/(2m) - \hbar\Delta_{\text{eff}} + E_R - i\hbar\gamma/2 \end{bmatrix} \tag{27}$$

and the latter by

$$H_B = \begin{bmatrix} 0 & -\hbar\Omega F(y)/2 \\ -\hbar\Omega F(y)/2 & 0 \end{bmatrix} \tag{28}$$

In the split operator method, the differential equation

$$i\hbar\frac{\partial}{\partial t}\varphi = (H_A + H_B)\varphi \tag{29}$$

with formal solution

$$\varphi(t) = \exp\left(-\frac{i(H_A + H_B)t}{\hbar}\right)\varphi(0) \tag{30}$$

is solved by approximating

$$\exp\left(-\frac{i(H_A + H_B)\Delta t}{\hbar}\right)\varphi \approx \exp\left(-\frac{iH_A\Delta t}{2\hbar}\right)\exp\left(-\frac{iH_B\Delta t}{\hbar}\right)\exp\left(-\frac{iH_A\Delta t}{2\hbar}\right)\varphi \tag{31}$$

which is accurate up to second order in Δt. The evolution involving H_A reduces to multiplications involving exponentials in momentum space while the evolution involving H_B proceeds in position space according to

$$\varphi_1(y, t+\Delta t) = \cos[\Omega F(y)\Delta t/2]\varphi_1(y,t) + i\sin[\Omega F(y)\Delta t/2]\varphi_2(y,t) \tag{32}$$

$$\varphi_2(y, t+\Delta t) = \cos[\Omega F(y)\Delta t/2]\varphi_2(y,t) + i\sin[\Omega F(y)\Delta t/2]\varphi_1(y,t) \tag{33}$$

A fast Fourier transform is used to convert the wave function between the spaces. By swapping alternately between the spaces and applying the appropriate evolution operator in each, a solution to the original equation may be obtained.

For efficiency, it is important to choose the time increment Δt appropriately. This is especially so in this problem, where the light profile $F(y)$ is rapidly varying with y. While the atomic wavepacket is far from the mirror, H_B is close to zero and large timesteps are possible. The stepsize must be reduced as the wavepacket approaches the mirror. An adaptive method for varying Δt was developed for this problem which proceeds as follows.

i) The error in a timestep may be estimated by calculating the difference between the two approximations to the Hamiltonian

$$\epsilon(\Delta t) = \frac{||\varphi_a - \varphi_b||}{||\varphi||} \tag{34}$$

where

$$\varphi_a = \exp\left(-\frac{iH_A\Delta t}{2\hbar}\right)\exp\left(-\frac{iH_B\Delta t}{\hbar}\right)\exp\left(-\frac{iH_A\Delta t}{2\hbar}\right)\varphi \tag{35}$$

$$\varphi_b = \exp\left(-\frac{iH_B\Delta t}{2\hbar}\right)\exp\left(-\frac{iH_A\Delta t}{\hbar}\right)\exp\left(-\frac{iH_B\Delta t}{2\hbar}\right)\varphi \tag{36}$$

The error is a quantity which scales as $(\Delta t)^3$. However, it is relatively expensive to compute as it requires six Fourier transforms rather than the two transforms for a normal step. Consequently, such an error estimate is only carried out approximately once every hundred normal steps.

ii) If the error estimate lies within the specified tolerance (chosen as 10^{-4} in the simulations), the values of all the variables are saved in case we need to restart the simulation back at this point. The next error estimate is scheduled after another hundred normal steps.

iii) If the error estimate is much smaller than (less than 0.2 times) the specified tolerance, the step size may be safely increased using the $(\Delta t)^3$ scaling law to give a target error of 0.7 times the tolerance.

iv) If on the other hand, the error estimate is greater than the specified tolerance, the results are discarded and the simulation is restarted from the last saved point. The step size is decreased using the $(\Delta t)^3$ scaling law to give a target error of 0.5 times the tolerance.

Using this strategy, it is found that adaptation takes place without too much time being spent on estimating errors and backtracking.

The split-operator method described above was used to simulate the system between spontaneous emission events. Each spontaneous emission is treated straightforwardly by using random numbers to give the direction of emission (θ, ϕ) of the photon and modifying wave functions as follows

$$\varphi_2(y,t)|_{\text{new}} = 0 \tag{37}$$

$$\varphi_1(y,t)|_{\text{new}} = \mathcal{N}\varphi_2(y,t)|_{\text{old}} \exp(-ik_{\text{L}} y \sin\theta\cos\phi) \tag{38}$$

This projects the atom into the ground state and applies a momentum kick in the y direction to simulate the recoil. $\mathcal{N}$ is a normalization constant chosen so that the new wavefunction is properly normalized after the jump. The component of the momentum kick along the z direction is $\hbar k_{\text{L}} \sin\theta \sin\phi$. This changes the velocity of the atom in the z direction which alters the Doppler shift Δ_{D} slightly. The new value of the Doppler shift is used for the subsequent simulation following the spontaneous emission. The ability to carry out a simulation with definite z momentum is an advantage of the quantum Monte Carlo formulation. For each realization, the z momentum is well-defined between spontaneous emissions. On the other hand, a density matrix approach would require us to keep track of a range of z momenta as this quantity varies across the ensemble.

6. Results.

In the numerical simulations, we employ normalized dimensionless variables as follows. Ω is the value of the Rabi angular frequency at the position where $F(y) = 1$. Angular frequencies and decay rates are normalized with respect to Ω, energies with respect to $\hbar\Omega$, lengths with respect to $\sqrt{\hbar/(m\Omega)}$ and momenta with respect to $\sqrt{m\hbar\Omega}$. We shall denote the dimensionless variables by tildes so that for example, $\tilde{\Delta}_{\text{D}} = \Delta_{\text{D}}/\Omega$ etc.

The atomic parameters selected were loosely based on those for the $5S_{1/2}$ to $5P_{3/2}$ transition of Rubidium [3] with a spontaneous emission linewidth of 6 MHz and a wavelength of 780 nm. If we choose $\Omega = 2\pi \times 30$ MHz, we find $\tilde{\gamma} = 0.2$. Using an evanescent wave $F(y) = F_0 \exp(-y/a)$ with exponential decay length of $a = 100$ nm, we find that $\tilde{a} = 50$. The initial kinetic energy in the y direction, namely $E_{\text{I}} = \hbar^2 k_{\text{I}}^2/(2m)$, is chosen so that the atomic de Broglie wavelength in the y direction is approximately twice the decay length. This gives $\tilde{E}_{\text{I}} = 2 \times 10^{-3}$ Physically, this corresponds to a y velocity component of about 2.4 $\text{cm}\,\text{s}^{-1}$. The z component of the velocity is adjusted to give an incident beam angle of 1 mrad. The photon wavenumber in dimensionless units is $\tilde{k}_{\text{L}} = 0.016$. In order to make the mirror reflect atoms incident in the ground state, the effective detuning $\Delta_{\text{eff}} = \Delta - \Delta_{\text{D}}$ is chosen to be positive with $\tilde{\Delta}_{\text{eff}} = 0.05$. These are the defaults used in the simulations and in the following we shall only explicitly mention the parameters which are not set to these values.

In figure 3, we show the interaction of a wavepacket of initial momentum uncertainty $\tilde{\sigma}_{\text{p}} = 0.002$ with the evanescent wave when the spontaneous emission $\tilde{\gamma}$ is set to zero. The dimensionless time is defined by $\tilde{t} = \Omega t$. The value of F_0 has been adjusted so that the classical turning point is located at $y = 0$. In the sequence of plots, we see that the wavepacket approaches the mirror and bounces off. During the bounce, there is interference between the components travelling towards and away from the mirror, leading to the oscillations in probability at intermediate times. In these plots, only the ground-state atomic population is shown, the excited state component being too small to be visible on the scale chosen. The concept of a quantum mechanical path for the particle is not well-defined but it is possible to plot

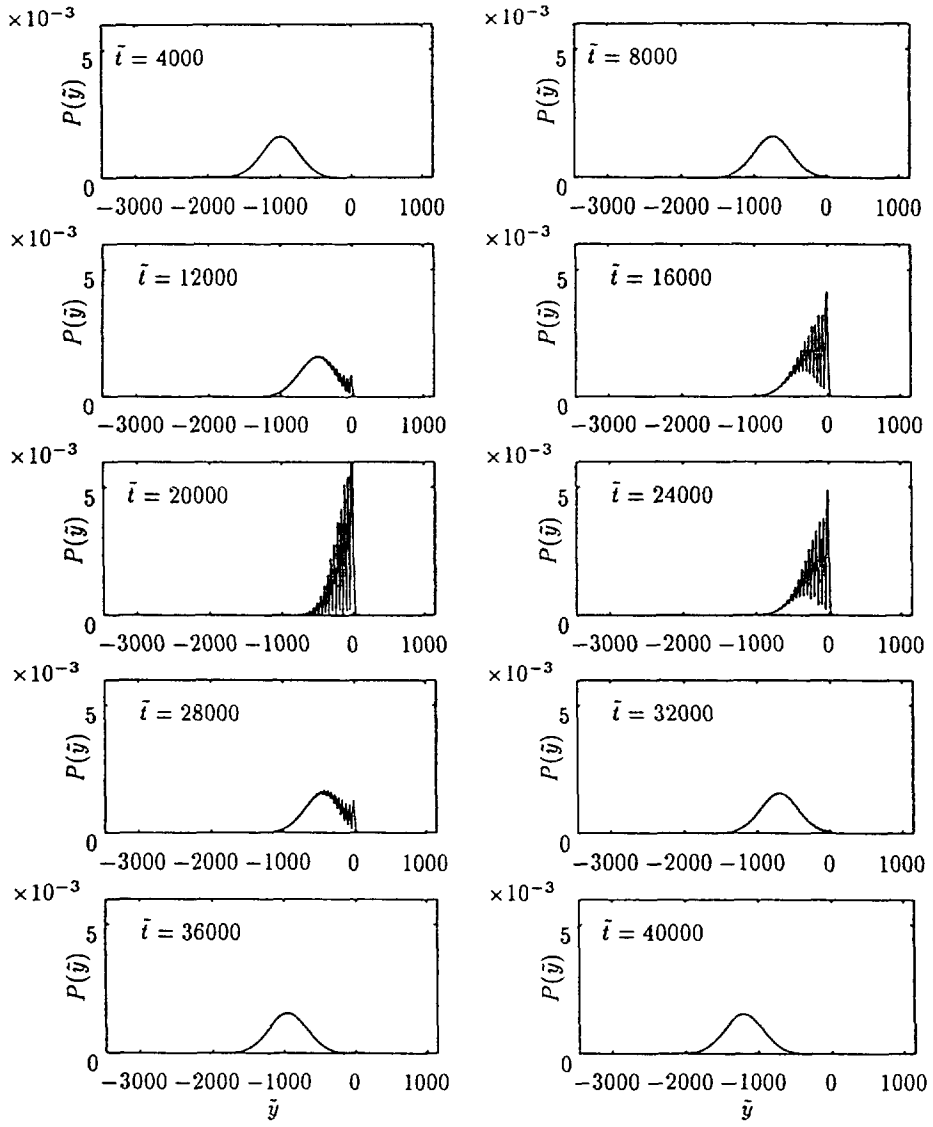

Fig. 3. — Sequence of position probability densities showing the interaction of a Gaussian wavepacket with an evanescent mirror in the absence of spontaneous emission. The position of the classical turning point is at $\tilde{y} = 0$. The dimensionless parameters used in the simulation are $\tilde{a} = 50$, $\Delta_{\text{eff}} = 0.05$, $\tilde{E}_{\text{I}} = 0.002$, $\tilde{k_{\text{L}}} = 0.016$ and $\tilde{\sigma}_{\text{p}} = 0.002$.

the expectation values $\langle\tilde{y}\rangle$ and $\langle\tilde{p}_y\rangle$ of the position and momentum as functions of time. In figure 4 the solid lines show the time evolution of these expectation values while the dashed lines show the semi-classical trajectory obtained by solving the classical equations of motion in the quasipotential $U_-(y)$. From this, it is clear that the quantum mechanical wave-packet does not penetrate the light field as deeply as the classical particle, largely due to the width of the wavepacket in position space. However, away from the turning point, there is good agreement

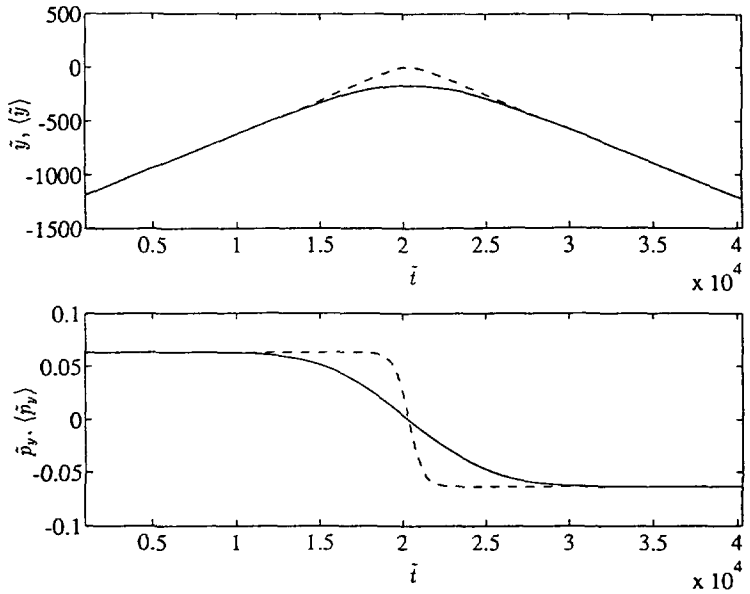

Fig. 4. — Comparison of quantum mechanical (solid lines) and classical (dashed lines) motion of an atomic wavepacket in the evanescent light field in the absence of spontaneous emission. The quantum mechanical graphs are of the mean position $\langle\tilde{y}\rangle$ and the mean y momentum $\langle\tilde{p}_y\rangle$ of the atomic wavepacket shown in figure 3. The classical results are found by integration of the equations of motion in for the $|-\rangle$ state quasipotential $U_-(y)$.

between the classical and quantum mechanical calculations.

In figure 5 we show five realizations of the semi-classical Monte Carlo algorithm for the default parameter values. We see that the plots of y as functions of t are necessarily continuous since the effect of a spontaneous emission is to impart a discontinuous momentum kick to the atom. This is appropriate when the atom may be treated as a point particle so that its wave nature is not important. When this is not the case, it is necessary to consider the external degrees of freedom quantum mechanically. In figure 6, the results of five realizations of the quantum Monte Carlo calculation are shown for the same parameters. As before, the expectation values $\langle\tilde{y}\rangle$ and $\langle\tilde{p}_y\rangle$ are shown. The most apparent difference between these plots and those for the semi-classical ones is that $\langle\tilde{y}\rangle$ exhibits discontinuities at the positions of the quantum jumps. Since in an evanescent wave, the force on the atom changes rapidly with position due to the approximately exponential shape of the quasipotentials, a process which changes the position of the atom within the evanescent field will lead to fluctuations in the force and a broadening of the outgoing momentum distribution. The extent of this broadening will depend on the size of the position jumps and the spatial scale on which the quasipotential varies. In the quantum-mechanical simulations, the continuous trajectories of the semi-classical picture are replaced by "paths" with discontinuous changes in the mean location of the wavepacket which leads to an additional broadening of the distribution of outgoing momentum when the average over many trajectories is considered.

In order to discover the origin of these jumps in position, we recall that in the quantum Monte-Carlo algorithm, the effect of a spontaneous emission (Eqs. (37) and (38)) is to set the new ground state to a normalized version of the old excited state. In figure 7, the composition of the wavepacket from the simulation which generated figure 3 at time $\tilde{t} = 2 \times 10^4$

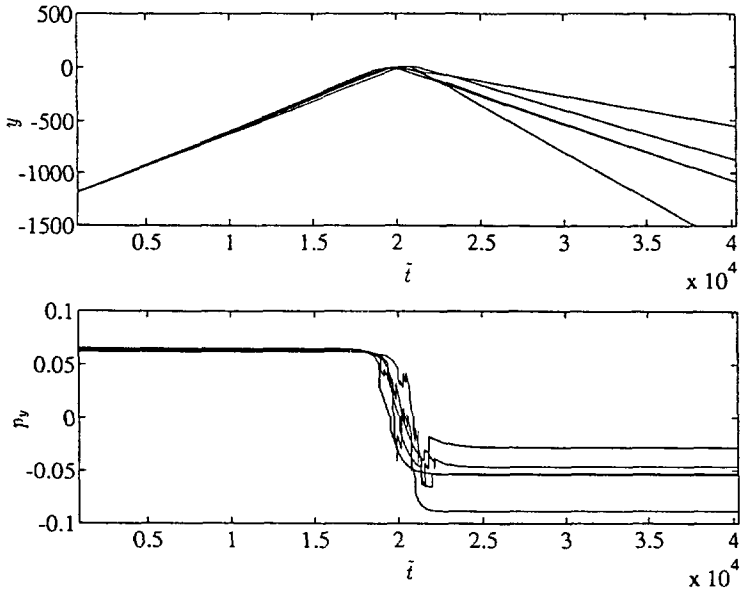

Fig. 5. — Graphs of (a) position and (b) momentum for five trajectories of the semi-classical Monte Carlo algorithm showing that the position is a continuous function of time but that the momentum changes discontinuously at the spontaneous emission events. Default parameter values were chosen, namely $\tilde{a} = 50$, $\Delta_{\text{eff}} = 0.05$, $\tilde{E}_{\text{I}} = 0.002$, $\tilde{\gamma} = 0.2$ $\tilde{k_{\text{L}}} = 0.016$ and $\tilde{\sigma}_{\text{p}} = 0.002$.

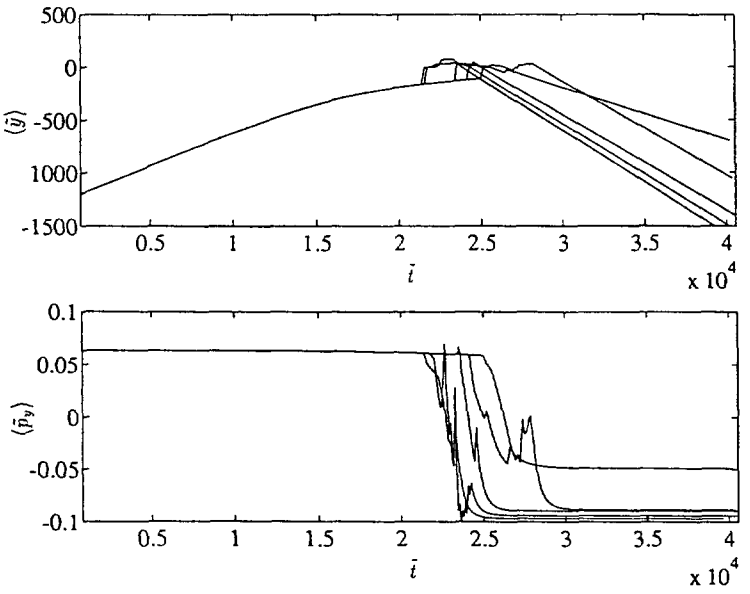

Fig. 6. — Graphs of mean position and mean momentum of the atomic wavepacket for five trajectories of the quantum Monte Carlo algorithm showing that the mean position has discontinuous jumps at the spontaneous emissions. The same parameter values were used as for figure 5.

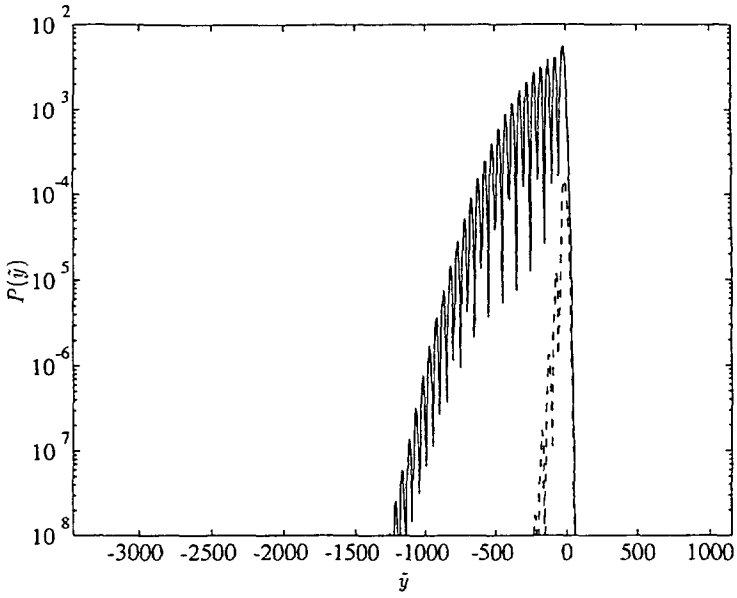

Fig. 7. — Position probability density functions of ground (solid line) and excited state (dashed line) populations in the wavepacket simulation of figure 3 at time $\tilde{t} = 2 \times 10^4$ when the wavepacket close to the middle of the bounce. The peak of the excited state population lies closer to the mirror that the peak of the ground state population.

(near the point of closest approach) is shown on a logarithmic scale. The solid line indicates the probability density of the ground state component and the dashed line that of the excited state component. It is clear that the peak for the excited state component is much closer to the mirror than that for the ground state since the excited state is in fact generated by interaction with the light. If a spontaneous emission was to occur at this time, the ground state wave function would be set to the excited state wave function, causing a discontinuous change in the expected value of the position. Although this particular simulation was done without the non-Hermitian part in the Hamiltonian, the same argument holds true in general.

We now compare the momentum distributions of the outgoing atoms as these are the experimentally measured quantities. In the quantum mechanical calculation, each realization shows how an incoming wavepacket with a certain momentum uncertainty evolves into an outgoing probability density for the momentum. According to the quantum Monte Carlo prescription, these probability densities must be averaged over many realizations to give the experimentally measurable distribution. In the following simulations, averages are taken over a hundred realizations. By contrast, in the semi-classical calculation, each realization traces the motion of an atom through the system, and the momentum remains well-defined throughout. Atoms entering with the same momentum can leave with different momenta due to different histories of spontaneous emission during the interaction. In order to compare the results with those of the quantum calculation however, the incoming atoms are chosen to have a range of momenta drawn from the same Gaussian distribution as that of the quantum mechanical wavepacket. From the two thousand realizations carried out for each semi-classical calculation, the collection of outgoing atomic momenta is converted into a probability density by plotting a histogram. For a finite number of realizations, this necessarily involves binning the data, the width of the

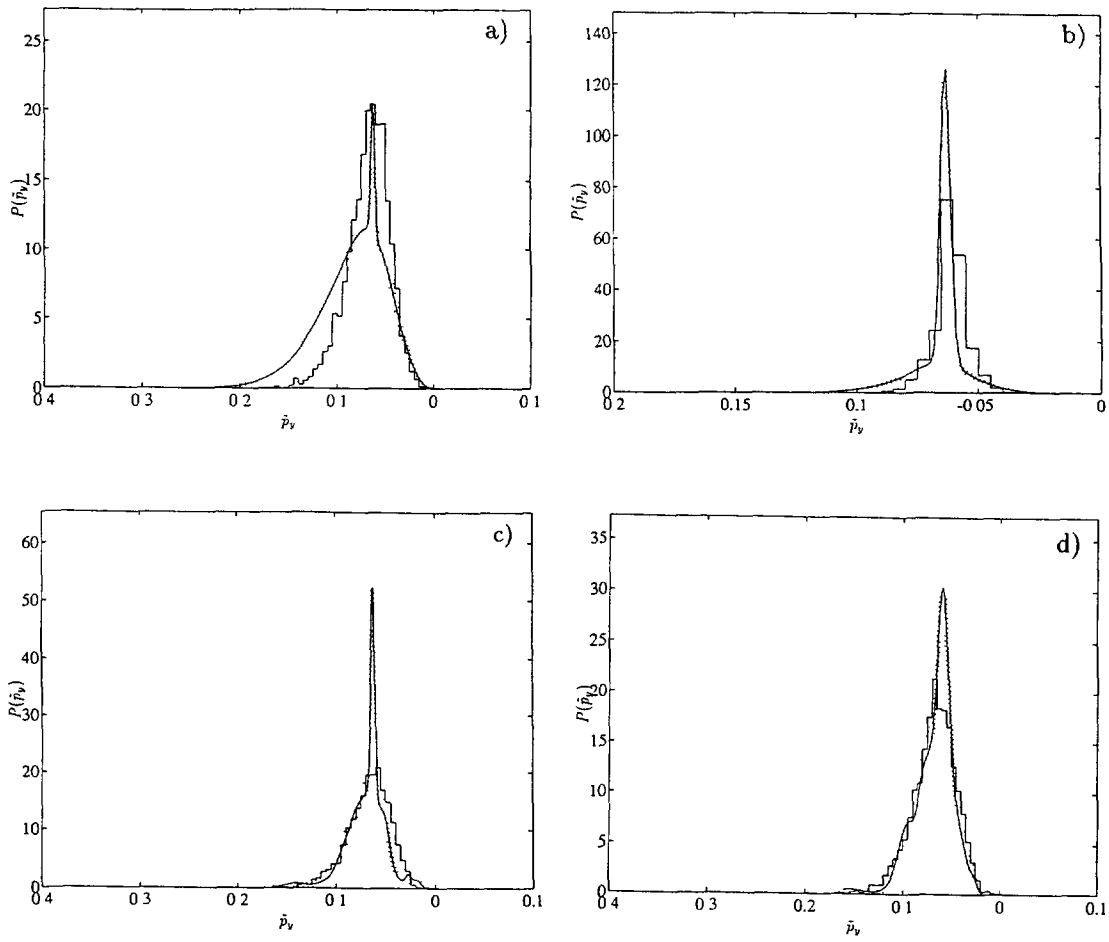

Fig. 8. — Outgoing momentum probability density (solid curve) calculated by averaging over 100 quantum Monte Carlo simulations. An indication of the accuracy of the simulation is given by the $\pm 1\sigma$ dotted curves. The solid staircase line is the result of averaging over approximately 2000 semi-classical Monte Carlo simulations. (a) Default parameter values have been used, namely $\tilde{a} = 50$, $\Delta_{\text{eff}} = 0.05$, $\tilde{E}_{\text{I}} = 0.002$, $\tilde{\gamma} = 0.2$ $\tilde{k_{\text{L}}} = 0.016$ and $\tilde{\sigma}_p = 0.002$. We find $\bar{n}_{QM} = 12.1 \pm 1.0$ and $\bar{n}_{SC} = 14.6 \pm 0.1$ are the average numbers of spontaneous emission for the quantum mechanical and classical simulations. (b) Default parameters except that $\tilde{\gamma} = 0.02$. We find $\bar{n}_{QM} = 2.8 \pm 0.3$ and $\bar{n}_{SC} = 3.91 \pm 0.05$. (c) Default parameters except that $\tilde{\gamma} = 0.02$ and $\tilde{a} = 500$. We find $\bar{n}_{QM} = 10.7 \pm 0.8$ and $\bar{n}_{SC} = 13.7 \pm 0.2$. (d) Default parameters except that $\tilde{\gamma} = 0.02$, $\tilde{a} = 500$ and $\tilde{p}_y = 0.005$. We find $\bar{n}_{QM} = 10.4 \pm 0.9$ and $\bar{n}_{SC} = 13.9 \pm 0.2$.

bins being a compromise between momentum resolution and having sufficient atoms within each bin to reduce the statistical fluctuations. In the following graphs, the bin width is chosen to be about the same as the width of the incoming momentum distribution as we do not expect variations on a smaller scale than this.

In the following figures, the probability density of the outgoing atomic momentum is plotted. The solid curve shows the result of the quantum mechanical calculation with the estimated one-sigma errors (based on the variance in the hundred realizations) being shown by the upper

and lower dotted curves. The result of binning the semi-classical Monte Carlo calculations is shown as the staircase plot. The area under the quantum and semi-classical plots have been adjusted to be equal to unity. Figure 8a is for the default parameter values and figure 8b is for the same parameters except that the spontaneous emission rate $\tilde{\gamma}$ has been reduced to 0.02. In both of these graphs, we see that the classical calculation gives a smaller spread of outgoing momentum than the quantum calculation. The initial half-width of the wavepacket is 250 dimensionless units which is large compared to the scale of the evanescent wave $\tilde{a} = 50$. The quantum mechanical results also show a sharper spike at the position of the "specular reflection" at which the outgoing momentum is equal to the incoming momentum. An atom is specularly reflected if it undergoes no spontaneous emissions during the bounce and so it appears that there are on average fewer spontaneous emissions in the quantum mechanical simulations than the quasi-classical simulations. The mean numbers of spontaneous emissions in the simulations are recorded in the figure captions and it is seen that this is indeed the case. This can be understood since the quantum mechanical wavepacket does not penetrate the light field as deeply as the classical turning point, and spontaneous emissions occur most frequently in regions where the atom is excited by the light.

In figure 8c, the parameters which differ from the default are $\tilde{\gamma} = 0.02$ and $\tilde{a} = 500$. The evanescent wave is now falling off over a larger range and so the change in the quasipotential across the wavepacket is much reduced. The approximation that the atom is a point particle holds more accurately in this regime and we see that there is indeed a better agreement between the classical and quantum calculations, although the spike for the specular reflection is still larger in the quantum mechanical case. If the incoming momentum distribution is wider, this spike would be broadened, leading to a better agreement. This is shown in figure 8d, where in addition, the initial momentum uncertainty has been increased from $\tilde{\sigma}_{\mathrm{p}} = 0.002$ to $\tilde{\sigma}_{\mathrm{p}} = 0.005$.

7. Summary.

In summary, the quantum Monte Carlo technique is useful for treating spontaneous emission in the regime of quantized internal and external motion as it straightforwardly models both the effects of momentum recoil on the atom as well the stochastic nature of the emission process without the use of large density matrices. The time-dependent solutions which it provides give insight into the mechanisms which cause broadening of the outgoing momentum distribution in the situation where the quantum mechanical atomic wave packet is so large that the quasipotentials vary significantly across the packet.

Acknowledgments.

We thank the New Zealand Foundation of Research, Science and Technology and the University of Auckland Research Committee for financial support.

References

[1] Cook R.J. and Hill R.K., *Opt. Commun.* **43** (1982) 258.

[2] Balykin V.I., Letokhov V.S., Ovchinnikov Yu. B. and Sidorov A.I., *Phys. Rev. Lett.* **60** (1988) 2137.

[3] Esslinger T., Weidemuller M., Hemmerich A. and Hansch T.W., *Opt. Lett.* **18** (1993) 450.

[4] Feron S., Reinhardt J., Le Boiteux S., Gorceix O., Baudon J., Ducloy M., Robert J., Miniatura Ch., Chormaic S., Haberland H. and Lorent V., *Opt. Commun.* **102** (1993) 83.

[5] SeifertW ., Adams C.S., Balykin V.I., Heine C., Ovchinnikov Yu. and Mlynek J., submitted to *Phys. Rev. A.*

[6] Hajnal J.V. and Opat G.I., *Opt. Commun.* **71** (1989) 119.

[7] Deutschmann R., Ertmer W. and Wallis H., *Phys. Rev. A* **47** (1993) 2169.

[8] Henkel C., Courtois J-Y., Kaiser R., Westbrook C. and Aspect A., to be published in *Laser Physics.*

[9] Dum R., Zoller P. and Ritsch H., *Phys. Rev. A* **45** (1992) 4879.

[10] Molmer K., Castin Y. and Dalibard J., *J. Opt. Soc. Am. B* **10** (1993) 524.

[11] Gardiner C.W., Parkins A.S. and Zoller P., *Phys. Rev. A* **46** (1992) 4363.

[12] Messiah A., Quantum Mechanics, Chap. 17 (North-Holland, Amsterdam, 1961)

[13] Dalibard J. and Cohen-Tannoudji C., *J. Opt. Soc. Am* **B2**(1985) 1707 .

[14] Kosloff R., *J. Phys. Chem.*, **92** (1988) 2087.